The Composition of the Highest Energy Cosmic Rays

J. Belz[a*]
for the High Resolution Fly's Eye Collaboration
[a] *University of Utah*
Salt Lake City, Utah 84112 U.S.A.

12 June, 2010

Abstract

We present recent results obtained from data collected by the High Resolution Fly's Eye (HiRes) observatory, focusing in particular on recent studies of the composition of the highest energy cosmic rays. The HiRes data are best explained by a light, primarily protonic composition above 1.6 EeV. We discuss the implications of the HiRes composition and spectral results for recent astrophysical models.

1 Introduction to HiRes; Recent Anisotropy Studies

The High Resolution Fly's Eye (HiRes) observatory, located in Dugway, Utah U.S.A. collected fluorescence light profiles from extensive air showers in monocular (1997-2006) and stereoscopic (1999-2006) modes. The HiRes-I (HiRes-II) "eye" observed elevation angles between 3° to 17° (3° to 31°) and recorded data via sample-and-hold (100 ns FADC) data acquisition electronics. The individual detector elements of the two eyes consisted of a 4.2 m^2 spherical mirror which focused light on a 256 pixel photomultiplier tube "camera". Each pixel in the camera covered approximately 1° of sky.

Stereoscopic reconstruction of air shower events proceeds by determining the *shower-detector plane* (SDP) of each eye, and then determining the shower core trajectory from the intersection of the two SDP's. This trajectory can then be reversed to obtain the arrival direction of the primary cosmic ray, collectively the arrival directions comprise a "skymap" which can be studied for evidence of anisotropy or arrival direction correlations with known astrophysical objects.

A recent HiRes anisotropy study focused on the search for correlations with Large Scale Structure (LSS) in the Northern Hemisphere. The expectation for the HiRes sky is obtained from the 2 micron all-sky survey (2MASS) [1]. Smearing was allowed to simulate galactic magnetic field effects, and Kolmogorov-Smirnov tests were performed under both the LSS-tracer and isotropic sky models.

The HiRes data are shown superimposed on LSS in Figure 1. Good agreement is found with the isotropic model, while the local LSS model yields poor agreement. HiRes excludes correlation at 95% c.l. for smearing angles less than 10° and energies greater than 40 EeV. More details of this study are contained in References [2] and [3]

2 Energy Spectrum Results

The next step in the reconstruction of air showers by the fluorescence technique is to form a "shower profile", using the event geometry and the fluorescence light yield [4] to infer the number

*email: belz@physics.utah.edu

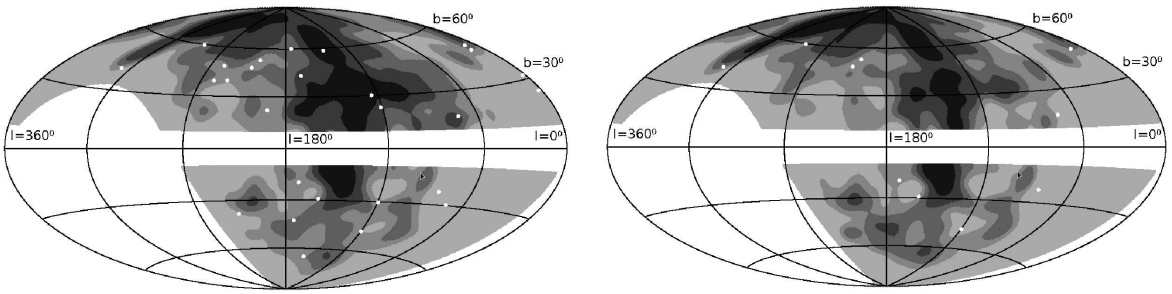

Figure 1: Hammer projection, galactic coordinates, of HiRes stereo arrival directions (white dots) superimposed on map of local large-scale structure. Darker gray indicates a higher matter density. The galactic plane and regions outside the HiRes field-of-view are excluded. *Left:* Threshold energy 40 EeV. *Right:* Threshold Energy 57 EeV.

of charged particles as a function of depth of the shower in the atmosphere. An example of a shower profile is shown in Figure 2 (left panel). The energy of an air shower, and hence of the cosmic ray primary, is inferred from the peak of this distribution or N_{max}.

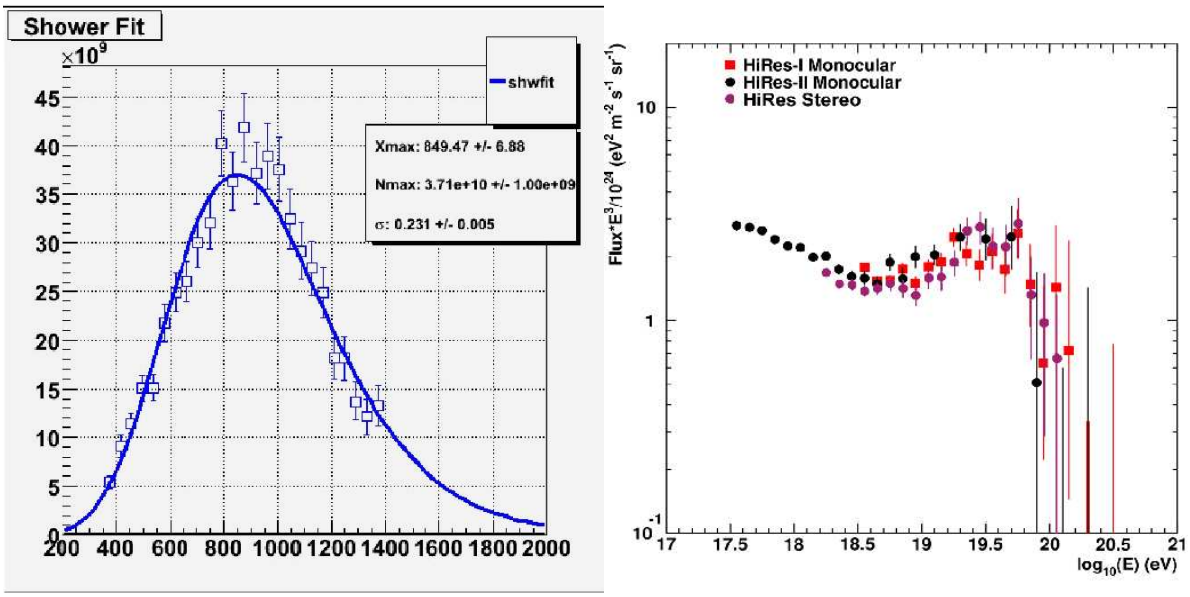

Figure 2: *Left:* Shower profile for typical HiRes event; charged particles versus depth in the atmosphere. *Right:* HiRes energy spectra compilation.

An energy spectrum is determined by dividing the event count in each bin by the *exposure* of the detector in units of area × solid angle × time. A compilation of the HiRes energy spectra are shown in Figure 2 (right panel), taken from References [5] and [6]. The HiRes spectra are characterized by two distinct features, the softening of the spectral index at approximately 3 EeV known as the "ankle", and the sharp suppression starting at about 30 EeV. The latter feature, first observed by HiRes in monocular mode is consistent with the so-called GZK [7] suppression first predicted in 1966. The GZK supression is due to the interaction of cosmic microwave background (CMB) photons with cosmic ray protons traversing cosmological distance scales. Protons, according to this model, lose energy via the photoproduction of pions. The presence of the GZK suppression is also therefore a hint as to the composition of the primary cosmic rays [8].

A second spectral signature of protons interacting with the CMB is a deficit due to e^+e^- pair production, predicted to occur at an energy of a few EeV [9] and thus consistent with the

energy spectrum ankle feature. An alternative model is that the ankle is the location of the transition from a heavy composition galactic component to a light extragalactic component [10]. Direct composition studies can play a decisive role in deciding between these models.

3 Composition Studies

A signature of primary cosmic ray composition which is accessible to fluorescence observatories such as HiRes is the distribution of *airshower maximum* or X_{max}. It can be shown [11, 12] that the average value of airshower maximum $<X_{max}>$ will depend logarithmically on the primary energy E and atomic mass A, *i.e.*

$$<X_{max}> \sim \left(\ln \frac{E}{E_c} - \ln A \right) + C \tag{1}$$

(where E_c is the critical energy and C is a constant) and that the *elongation rate* $d <X_{max}> / d \log E$ will be constant for unchanging primary compositions

$$\frac{d <X_{max}>}{d \log E} \sim \left(2.3 - \frac{d \ln A}{d \log E} \right). \tag{2}$$

Further, to first order, a nucleus-induced shower may be thought of as a superposition of showers induced by single nucleons. Therefore due to averaging effects we also expect the width of the X_{max} distribution at a given energy to be sensitive to the atomic mass of the primary.

The implied constant of proportionality and C in Equation 1 are both dependent on the details of hadronic interaction models at extrapolated energies. Hence there is no model-independent way to determine composition via X_{max} (although the prediction that a *change* in mean A must be accompanied by a change in the elongation rate is model independent). In practice, the models used are extensive air shower Monte Carlo programs. That is, simulated airshowers are mandatory for composition studies as is understanding detector response to these simulated airshowers.

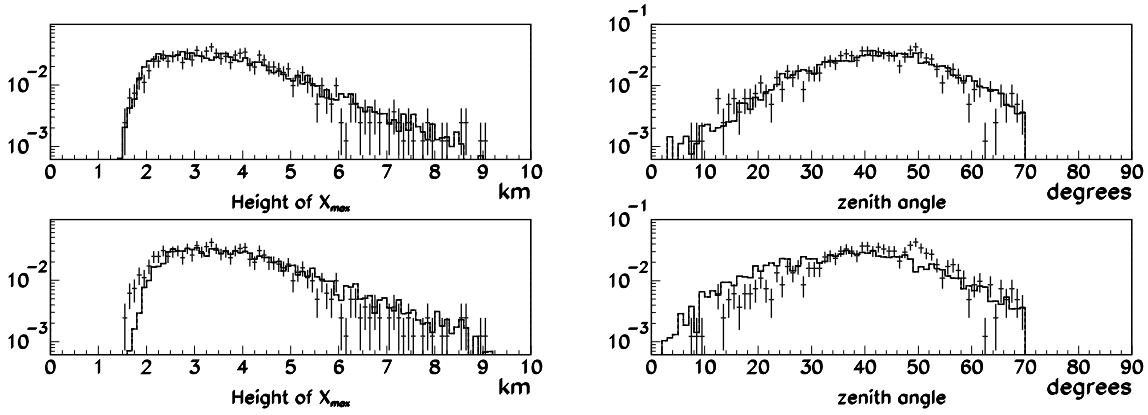

Figure 3: *Left:* Top plot, comparison of HiRes data (points) and QGSJET-II proton Monte Carlo, height of X_{max} above ground level. Bottom plot, same variable, comparison of HiRes data and QGSJET-II iron Monte Carlo. *Right:* Top plot, comparison of HiRes data (points) and QGSJET-II proton Monte Carlo, zenith angle of air shower. Bottom plot, same variable, comparison of HiRes data and QGSJET-II iron Monte Carlo.

HiRes uses a full detector simulation to model the response to simulated airshowers. This simulation incorporates an hourly atmospheric database, ray tracing of fluorescence light from

the shower to the mirrors and camera, simulated photomultiplier response and trigger, and subjecting the simulated events to the full analysis chain which is applied to the data.

To confirm that the detector response to air showers is well understood, in particular to check that various effects which could bias the measurement of mean X_{max} are under control, we conduct a systematic program of data versus Monte Carlo comparisons in distributions of interest. Of particular concern are limitations on the field of view of the cameras, which if not understood could bias both the mean value of X_{max} and the width of the distribution. Figure 3 includes comparisons of the HiRes stereo data with Monte Carlo events using the CORSIKA [13] simulation package. For comparisons presented here, we use the QGSJET-II [14] high-energy hadronic interaction model, however similar studies were also conducted using QGSJET01 [15] and SIBYLL [16].

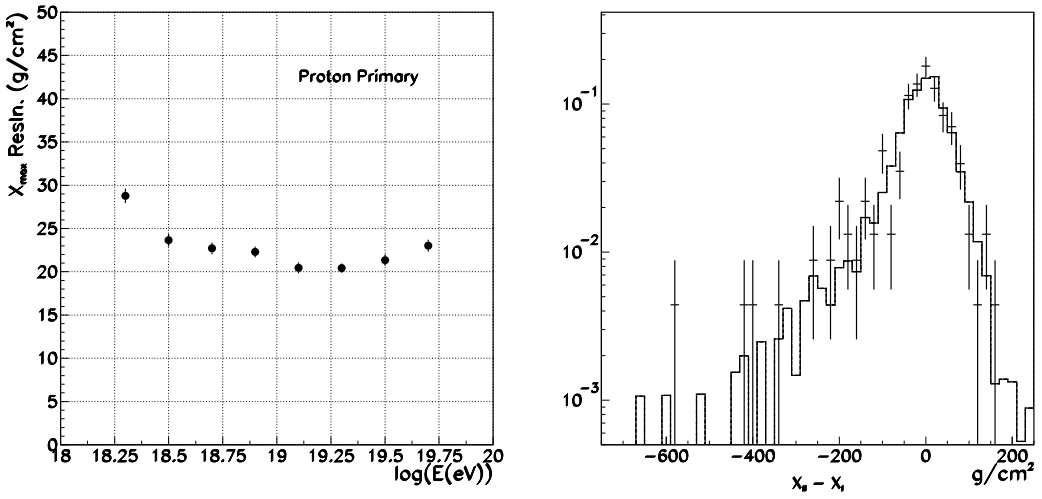

Figure 4: *Left:* X_{max} resolution (Gaussian fit) for QGSJET-II proton Monte Carlo. *Right:* Difference between HiRes-II (X_{II}) and HiRes-I (X_I) X_{max} for HiRes stereo data (points) overlaid with QGSJET-II proton Monte Carlo. X_{max} bracketing by HiRes-I is required.

Detector resoltion in the X_{max} variable is calculated using Monte Carlo airshowers and confirmed using stereo data, as shown in Figure 4. The resolution of better than 25 g/cm^2 over most of the HiRes energy range is more than adequate for differentiating between various particle species. The X_{max} distributions for HiRes stereo data are compared with Monte Carlo in Figure 5, and in energy bins in Figure 6.

Figure 7 contains the final graphs showing mean X_{max} and the width of the X_{max} distribution as a function of energy, including comparisons with various hadronic models. Using a linear fit to the $<X_{max}>$ data with a $\chi^2 = 5.2/6$ d.f. we measure a constant elongation rate of 48 ± 6 g/cm^2/decade.

As demonstrated in the figures shown here, the data is best modeled by QGSET-II protons, in all distributions. The absolute value of mean X_{max} is bracketed by QGSJET01 and QGSJET-II, and the elongation rate is consistent with either. Within the SIBYLL model the data falls between protons and helium, suggesting a light, mixed composition. The constant elongation rate suggests the unlikely scenario that this mixture is unchanging (or at best, steadily changing) over two orders of magnitude. Such a mixed model is also inconsistent with either interpretation of the energy spectrum ankle: The pair-production model requires that protons dominate, while the galactic-to-extragalactic transition model would imply that the transition is occurring with a constant mixed composition. Finally, the width of the X_{max} distributions is consistent with a proton interpretation. A more detailed description of the HiRes detector and composition analysis is contained in Reference [17].

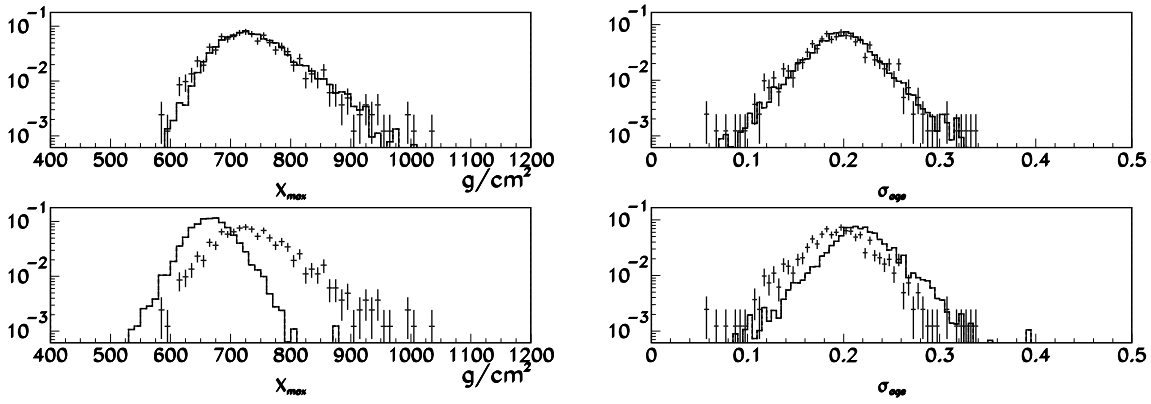

Figure 5: *Left:* Top plot, comparison of HiRes data (points) and QGSJET-II proton Monte Carlo, depth of shower maximum (X_{max}). Bottom plot, same variable, comparison of HiRes data and QGSJET-II iron Monte Carlo. *Right:* Top plot, comparison of HiRes data (points) and QGSJET-II proton Monte Carlo, σ of Gaussian-in-age fit. Bottom plot, same variable, comparison of HiRes data and QGSJET-II iron Monte Carlo.

4 Conclusions

The HiRes spectral results are consistent with a protonic composition. The location of the high-energy cutoff and its shape are consistent with the GZK cutoff due to proton interactions with the CMB. The ankle feature is in the correct location and has the correct shape for to be consistent with proton-induced CMB pair production.

The observed data, in all distributions, are consistent with pure protons within the QGSJET01 and QGSJET-II high energy hadronic interaction models. The observed constant elongation rate suggest a constant light composition above 1.6 EeV, making the SIBYLL mixed model unlikely. Further, the unchanging elongation rate rules out the ankle as the site of the galactic-to-extragalactic transition.

In summary, the HiRes spectral and composition results can be explained by a simple model: Cosmic rays above 1 EeV are protons of extragalactic origin. The high-energy spectrum is shaped by interaction of these protons with the cosmic microwave background.

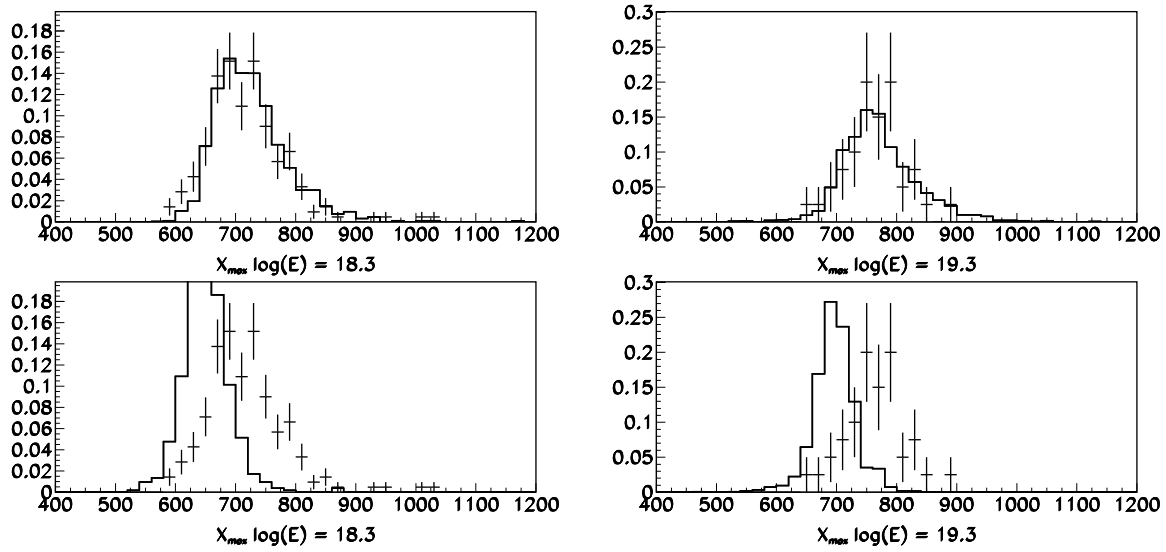

Figure 6: *Left:* Top plot, comparison of HiRes data (points) and QGSJET-II proton Monte Carlo, depth of shower maximum (X_{max}), $\log E = 18.3$. Bottom plot, same variable, comparison of HiRes data and QGSJET-II iron Monte Carlo. *Right:* Top plot, comparison of HiRes data (points) and QGSJET-II proton Monte Carlo, depth of shower maximum (X_{max}), $\log E = 19.3$. Bottom plot, same variable, comparison of HiRes data and QGSJET-II iron Monte Carlo.

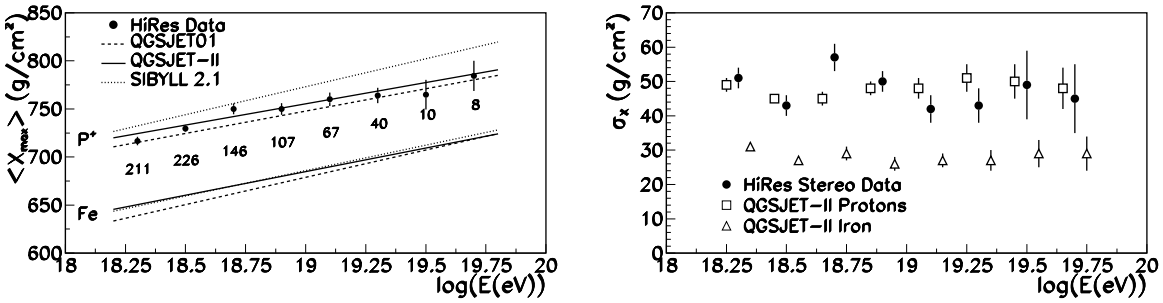

Figure 7: *Left:* HiRes stereo $<X_{max}>$ compared with the predictions for QGSJET01, QGSJET-II and SIBYLL protons and iron after full detector simulation. The number of events in each energy bin is displayed below the data point. *Right:* Results of fitting HiRes stereo data X_{max} distribution to Gaussian truncated at $2 \times$ RMS (black points). Superimposed are expectations based on QGSJET-II proton (squares) and iron (triangles) Monte Carlo. Monte Carlo points are shown with small offsets in energy to provide separation.

Acknowledgments

This work is supported by US NSF grants PHY-9321949, PHY-9322298, PHY-9904048, PHY-9974537, PHY-0098826, PHY-0140688, PHY-0245428, PHY-0305516, PHY-0307098, and by the DOE grant FG03-92ER40732.We gratefully acknowledge the contributions from the technical staffs of our home institutions. The cooperation of Colonels E. Fischer, G. Harter and G. Olsen, the US Army, and the Dugway Proving Ground staff is greatly appreciated.

References

[1] J. Huchra *et al.*, **https://www.cfa.harvard.edu/∼huchra/2mass/** (2010).

[2] P. Tinkakov, proceedings of this conference.

[3] R. Abbasi *et al.*, *Ap. J. Lett.* **713** (2010).

[4] R. Abbasi *et al.*, *Astropart. Phys.* **29** 77 (2008).

[5] R. Abbasi *et al.*, *Phys. Rev. Lett.* **100** (2008).

[6] R. Abbasi *et al.*, *Astropart. Phys.* **32** (2010).

[7] K. Greisen, *Phys. Rev. Lett.* **16** 748 (1966).
G.T. Zatsepin and V.A. Kuzmin, *JETP Lett.* **4** 78 (1966).

[8] V. Berezinsky *et al.*, *Phys. Rev.* **D74** (2006).

[9] R. Aloisio *et al.*, *Astropart. Phys.* **27** (2007).

[10] A. Hillas, *Nucl. Phys. Proc. Supp.* **136** (2004).

[11] W. Heitler, *The Quantum Theory of Radiation* (Oxford University Press, 1954).

[12] J. Matthews, *Astropart. Phys.* **22** 387 (2005).

[13] D.Heck and J.Knapp, *Tech. Rep. Forschungzentrum Karlsruhe* (1998).

[14] S.Ostapchenko, *Nucl. Phys. Proc. Suppl.* **151B** 143 (2006).

[15] N.Kalmykov and S.Ostapchenko, *Phys. Atom. Nucl.* **56** 346 (1993).

[16] R.Fletcher *et al.*. *Phys. Rev.* **D50** 5701 (1994).
R.Engel *et al.*, *Proc. 26th Intl. Cosmic Ray Conference* (Salt Lake City, Utah, U.S.A. 1999).

[17] R. Abbasi *et al.*, *Phys. Rev. Lett.* **104** (2010).